

processes for ligands.¹ Such processes appear to be quite common in bromide systems and may reflect the greater stability of bromide bridging ligands in contrast to chloride. The quantitative results of the

present work confirm the speculation of Grinberg and Shagisultanova,⁷ which was based on very fragmentary evidence, that bromide ligands were traded between *trans*-Pt(NH₃)₂Br₂ and PtBr₄²⁻.

CONTRIBUTION FROM THE DEPARTMENTS OF CHEMISTRY AND PHYSICS,
UNIVERSITY OF MAINE, ORONO, MAINE 04473

Sharp-Line Luminescence and Absorption Spectra of the Tetrachloroplatinate(II) Ion Doped in Single Crystals of Cesium Hexachlorozirconate(IV) at 4°K

By HOWARD H. PATTERSON,*^{1a} JOHN J. GODFREY,^{1a} AND S. M. KHAN^{1b}

Received June 13, 1972

The optical spectrum of the tetrachloroplatinate(II) ion in single crystals and as an impurity in Cs₂ZrCl₆ has been measured at 4°K. First, sharp-line luminescence has been observed between 19,450 and 23,190 cm⁻¹ for the tetrachloroplatinate(II) ion in mixed crystals and assigned to the transition $\Gamma_5(^3B_{1g}) \rightarrow \Gamma_1(^1A_{1g})$. Most of the detailed vibronic structure can be assigned to odd vibrational modes of the PtCl₄²⁻ complex in its ground electronic state. Franck-Condon analysis of the luminescence spectrum has shown that the Pt-Cl equilibrium distance in the $\Gamma_5(^3B_{1g})$ excited state is 0.16 Å greater than in the ground state. Second, the d-d transition $\Gamma_1(^1A_{1g}) \rightarrow \Gamma_2(^1A_{2g})$ has been observed between 24,800 and 28,000 cm⁻¹ with detailed vibronic structure. Finally, a crystal field analysis within the d⁸ manifold fits the available experimental maxima data with an rms deviation of about 100 cm⁻¹ for the parameters $F_2 = 1406$, $F_4 = 54$, $SO = 1013$, $\Delta_1 = 25,961$, $\Delta_2 = 41,821$, and $\Delta_3 = 33,184$ cm⁻¹.

Introduction

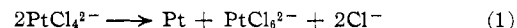
In order to eliminate metal-metal interactions present in pure single crystals we have grown single mixed crystals of the 5d⁸ square-planar tetrachloroplatinate(II) ion doped as an impurity in the host lattice cesium hexachlorozirconate(IV) and measured the optical spectrum of the mixed crystals at liquid helium temperature. Since the complex ions in the mixed crystal are isolated from each other and at 4°K reduced to their zero-point vibrational motion, sharply resolved spectra for some transitions can be obtained. The optical data can be analyzed to yield information about the vibrational modes of the excited electronic states and the proper assignment of these states.

Optical measurements for the PtCl₄²⁻ complex until now have consisted of solution and crystal studies. Martin, Tucker, and Kassman² and Mortensen³ have studied the polarized optical absorption spectrum of single K₂PtCl₄ crystals at liquid helium temperature and were able to assign the transition at 26,000 cm⁻¹ as $\Gamma_1(^1A_{1g}) \rightarrow \Gamma_2(^1A_{2g})$. McCaffery, Schatz, and Stephens⁴ have studied the magnetic circular dichroism of a single K₂PtCl₄ crystal at 4°K. Their results strongly suggest that the transition observed at 30,000 cm⁻¹ can be assigned as $\Gamma_1(^1A_{1g}) \rightarrow \Gamma_5(^1E_g)$. Finally, Webb and Rossiello⁵ have observed luminescence for K₂PtCl₄ at 77°K with a peak maximum at 12,700 cm⁻¹ and a half-width of 2400 cm⁻¹.

Experimental Section

Single K₂PtCl₄ Crystals.—The K₂PtCl₄ used for this study was purchased from Alfa Inorganics, Inc. In a first attempt to grow large crystals of K₂PtCl₄, an acidified solution of the platinum

complex was heated to 70° and then allowed to cool slowly back to room temperature. However, it was observed that upon heating the solution black particles began to form and upon cooling such a solution, a small-grained yellow precipitate could be obtained even if the volume of the solution was such that the orange-red K₂PtCl₄ should not precipitate. The yellow substance dissolved slowly in a high concentration of HCl. The black particles were suspected to be platinum metal and the yellow precipitate fitted the description of K₂PtCl₆. The reaction responsible for these products would be



To prevent reaction 1 from occurring a different method for growing K₂PtCl₄ crystals was devised. A saturated solution of K₂PtCl₄ with a high concentration of KCl at room temperature was allowed to evaporate in a desiccator with concentrated H₂SO₄ as the drying agent. This method had a twofold advantage over the original method: (a) the condensation was performed without the addition of heat which seemed to hasten the disproportionation; (b) the excess chloride ion concentration decreased the amount of disproportionation. Using this method large crystals (1 × 1 × 4 mm) were harvested after 2 or 3 days.

Preparation of Cs₂PtCl₄-Cs₂ZrCl₆ Mixed Crystals.—The preparation of cesium hexachlorozirconate(IV) has been described in earlier publications.^{6,7} The mixed crystals of Cs₂PtCl₄-Cs₂ZrCl₆ were prepared by placing a weighed amount of the platinum complex with Cs₂ZrCl₆ in an evacuated Vycor tube. The mole per cent of the platinum complex was 0.1–1.0%. The Vycor tube was dropped through a 24-in. vertical furnace at 800° in about 2 days' time. Large clear mixed crystals were obtained. Sections of the mixed crystals for optical studies were cleaved with a razor blade. It is known that the ZrCl₆²⁻ complex does not absorb up to 45,000 cm⁻¹;^{6,8} therefore, the spectra reported here cannot be due to the host material.

Spectroscopic Measurements.—The crystals were mounted in an Air Products and Chemicals Inc. Model AC-3L Cryo-Tip. This instrument provided temperatures down to the liquid helium range using liquid nitrogen and gaseous hydrogen and helium. The temperature was measured with a chromel-constantan thermocouple.

The optical spectra were recorded with a McPherson 1-m

(1) (a) Department of Chemistry. (b) Department of Physics.
(2) D. S. Martin, M. A. Tucker, and A. J. Kassman, *Inorg. Chem.*, **4**, 1682 (1965).
(3) O. S. Mortensen, *Acta Chem. Scand.*, **19**, 1500 (1965).
(4) A. J. McCaffery, P. N. Schatz, and P. J. Stephens, *J. Amer. Chem. Soc.*, **90**, 5730 (1968).
(5) D. L. Webb and L. A. Rossiello, *Inorg. Chem.*, **9**, 2622 (1970).

(6) P. B. Dorain, H. H. Patterson, and P. C. Jordan, *J. Chem. Phys.*, **49**, 3845 (1968).

(7) H. H. Patterson and J. L. Nims, *Inorg. Chem.*, **11**, 520 (1972).

(8) B. J. Brisdon, T. E. Lester, and R. A. Walton, *Spectrochim. Acta, Part A*, **23**, 1969 (1967).

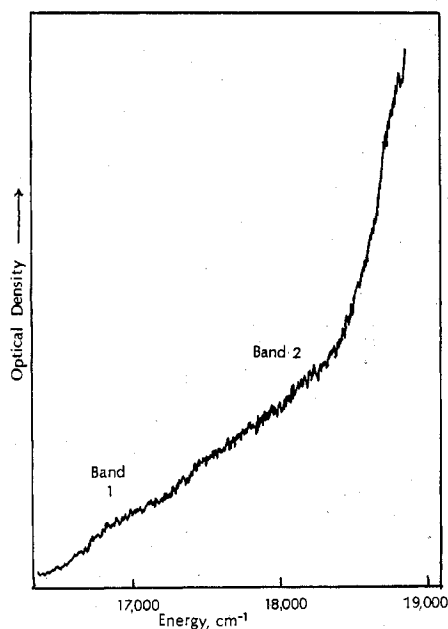


Figure 1.—Microphotometer tracing of a photographic plate showing absorption bands 1 and 2 in the tail of band 3 for a K_2PtCl_4 single crystal.

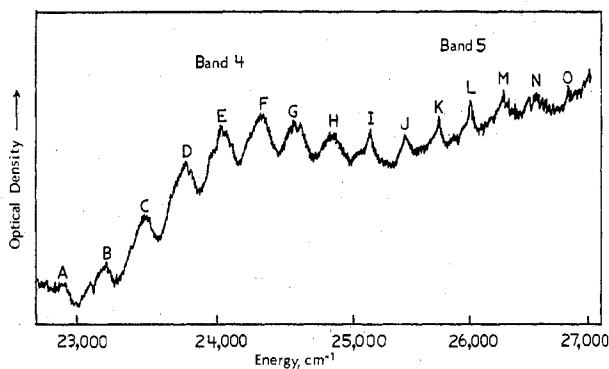


Figure 2.—Microphotometer tracing of a photographic plate showing vibronic detail in bands 4 and 5 for a K_2PtCl_4 single crystal.

Model 2051 monochromator on photographic plates. The plate factor was 8.25 \AA/mm in the first order. A high-pressure xenon lamp was used as the light source. All observed spectra were calibrated *vs.* iron arc spectra.

In our first experiments the optical spectra were obtained with a Bausch and Lomb Research dual grating spectrograph. The plate factor was 8.25 \AA/mm in the first order. The crystals were glued to a brass holder and immersed in liquid helium. The same spectrum was obtained at 4°K in both types of experiments.

Experimental Results

Single K_2PtCl_4 Crystal Spectrum at 4°K .—Figure 1 shows bands labeled 1 and 2 in the tail of band 3. These absorptions are weak and broad with maxima around $17,000$ and $18,000 \text{ cm}^{-1}$, respectively. No vibronic structure is evident. Band 3 extends from $19,500$ to $21,000 \text{ cm}^{-1}$ with a maximum at $20,500 \text{ cm}^{-1}$. Bands 4 and 5 are shown in Figure 2. Band 4 shows a maximum at $24,300 \text{ cm}^{-1}$ while band 5 has a maximum at $26,300 \text{ cm}^{-1}$. There is vibronic structure for each of these two bands. The energies of the various peaks are given in Table I. The average spacing between peaks A–G is slightly less than the spacing between peaks H–O. Band 6 extends from $27,000$ to $31,500$

TABLE I

OBSERVED OPTICAL ABSORPTION DATA FOR K_2PtCl_4 SINGLE CRYSTAL IN $22,800$ – $26,800\text{-cm}^{-1}$ ENERGY REGION AT 4°K

Peak	Energy, cm^{-1}	Assignment ^a
A	22,880	$\Gamma_5(^3B_{1g}) + \nu_{\text{odd}}$
B	23,170	$+ (\nu_{\text{odd}} + \nu_1)$
C	23,450	$+ (\nu_{\text{odd}} + 2\nu_1)$
D	23,740	$+ (\nu_{\text{odd}} + 3\nu_1)$
E	24,020	$+ (\nu_{\text{odd}} + 4\nu_1)$
F	24,300	$+ (\nu_{\text{odd}} + 5\nu_1)$
G	24,580	$+ (\nu_{\text{odd}} + 6\nu_1)$
H	24,850	$\Gamma_2(^1A_{2g}) + \nu_6^b$
I	25,140	$+ (\nu_6 + \nu_1)$
J	25,430	$+ (\nu_6 + 2\nu_1)$
K	25,720	$+ (\nu_6 + 3\nu_1)$
L	26,000	$+ (\nu_6 + 4\nu_1)$
M	26,290	$+ (\nu_6 + 5\nu_1)$
N	26,570	$+ (\nu_6 + 6\nu_1)$
O	26,860	$+ (\nu_6 + 7\nu_1)$

^a A transition is denoted by the excited state to which the transition occurs. ^b Based upon mixed-crystal analysis in this energy region.

cm^{-1} with a maximum at $29,600 \text{ cm}^{-1}$ and is a broad absorption band with no obvious vibronic structure. At $33,000 \text{ cm}^{-1}$ can be seen the start of a broad absorption band which we label band 7. In Table II our single-crystal optical results are summarized. The results of Martin, Tucker, and Kassman² and Mortensen³ are also given.

Mixed Cs_2PtCl_4 – Cs_2ZrCl_6 Crystal Spectrum at 4°K .—Spectral studies of Cs_2PtCl_4 doped in the host Cs_2ZrCl_6 have revealed two regions of interest. A sharply structured absorption band has been observed in the $24,800$ – $28,000\text{-cm}^{-1}$ region and sharp-line luminescence has been measured in the $19,450$ – $23,190\text{-cm}^{-1}$ region.

The observation of the $24,800$ – $28,000\text{-cm}^{-1}$ band was important in demonstrating that Cs_2PtCl_4 was present in the mixed crystal after the Cs_2PtCl_4 and the Cs_2ZrCl_6 had been melted together at 800° . Figure 3 shows how the vibronic peaks of the $PtCl_4^{2-}$

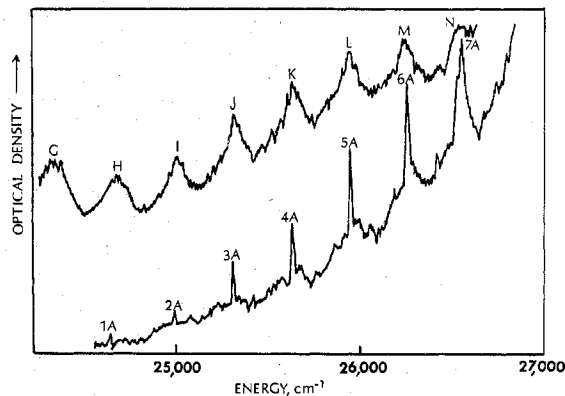


Figure 3.—A comparison of the $\Gamma_1(^1A_{1g}) \rightarrow \Gamma_2(^1A_{2g})$ absorption spectrum in a single K_2PtCl_4 crystal and in a Cs_2PtCl_4 – Cs_2ZrCl_6 crystal.

complex in the mixed crystal compare with the peaks in single crystals of K_2PtCl_4 . The peaks for the mixed crystal are all shifted about 50 cm^{-1} from the peaks of the single K_2PtCl_4 crystal. The energy separations between the peaks in the two systems agree very well. The most significant difference between the two spectra is the sharpness of the absorption lines. The mixed crystals give very sharp spectral peaks whereas the single crystals give only broad humps. There can be

TABLE II
 SUMMARY OF LIQUID HELIUM ABSORPTION DATA FROM SINGLE K_2PtCl_4 CRYSTAL STUDIES

Band No.	Our data ν , cm^{-1} (ν_{max} , cm^{-1})	Mortensen data ^a			Martin data ^b		
		ν_{max} , cm^{-1}	Polarization	Oscillator strength $\times 10^4$	ν_{max} , cm^{-1}	Polarization	Oscillator strength $\times 10^4$
1	16,600–17,300 (17,000)	17,190	<i>z</i>	0.03	17,000		
		16,930	<i>xy</i>	0.005			
2	17,400–18,500 (18,000)	18,100	<i>xy</i>	0.09	18,000	<i>xy</i>	0.2
3	19,500–21,000 (20,500)	20,660	<i>z</i>	0.77	20,600	<i>z</i>	1.2
		20,810	<i>xy</i>	0.73			
4	22,880–24,580 (24,300)	23,940	<i>z</i>	0.13	24,100	<i>z</i>	0.4
		24,000	<i>xy</i>	0.35			
5	24,850–26,860 (26,300)	26,050	<i>xy</i>	1.6	26,300	<i>xy</i>	3.2
6	27,500–31,500 (29,600)	29,900	<i>z</i>	4.3	29,800	<i>z</i>	7.1
		29,250	<i>xy</i>	3.6			
7	33,000–	36,500			29,200	<i>xy</i>	5.0

^a Reference 3. ^b Reference 2.

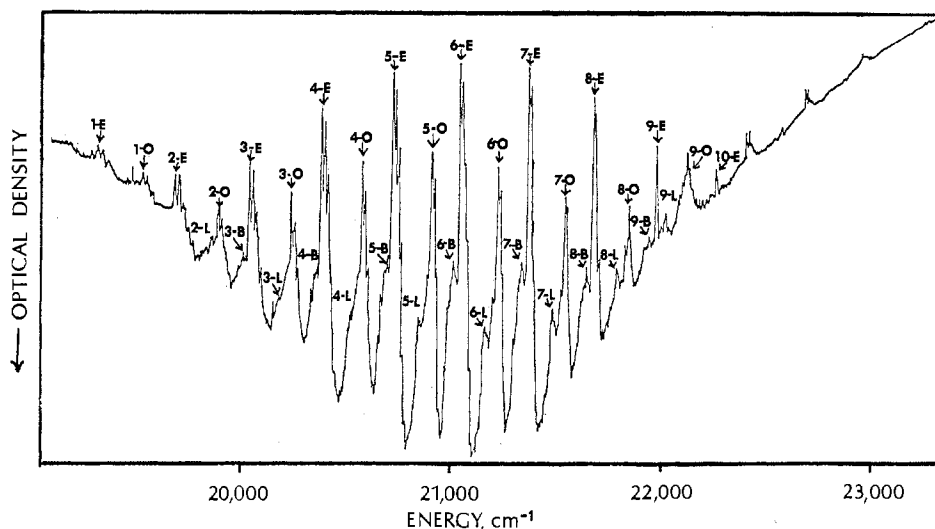


Figure 4.—Microphotometer tracing of a photographic plate showing the luminescence spectrum of a Cs_2PtCl_4 - Cs_2ZrCl_6 single crystal at $4^\circ K$.

little doubt that tetrachloroplatinate(II) ions are present in the mixed crystals; however, the possibility still exists that impurities may be present.

A sharp-line emission spectrum was observed between 19,450 and 23,190 cm^{-1} for $PtCl_4^{2-}$ in Cs_2ZrCl_6 . The luminescence spectrum observed at $4^\circ K$ is given in Figure 4. The spectrum consists of two major sets of peaks labeled E and O, the E peaks of more intensity than the O peaks. Each of these peaks is split with the magnitude of the splitting increasing toward the lower energy end of the spectrum. The E peaks start with low intensity, increase to a maximum around 21,000 cm^{-1} , then decrease until they disappear beyond 22,363 cm^{-1} . In contrast, the O peaks begin at about the same energy as the E peaks, reach their maximum about the same energy, and appear to be decreasing until peak 9O where the intensity increases and then gradually decreases until the peaks disappear beyond 23,500 cm^{-1} , about 1000 cm^{-1} past the point where the E peaks terminate. Two other noteworthy phenomena occur: (1) peak 9O is extremely broad and does not have the same general appearance as the other peaks; and (2) the splittings for the O peaks decrease before 9O, then suddenly increase noticeably at peak 9O at which point they decrease again in going to higher energies. For these reasons it is assumed that the

O peaks terminate at 9O and the other peaks present at higher energies must be due to another electronic transition.

Discussion

Crystal Field Model.—Crystallographic studies have shown that the $PtCl_4^{2-}$ ion possesses D_{4h} symmetry in single K_2PtCl_4 crystals. Pt^{2+} has a $5d^8$ configuration and when placed in a strong crystal field with square-planar symmetry the following electronic states result: $^1A_{1g}(4)$, $^1A_{2g}(1)$, $^3A_{2g}(2)$, $^1B_{1g}(2)$, $^3B_{1g}(1)$, $^1B_{2g}(2)$, $^3B_{2g}(1)$, $^3E_g(3)$, and $^1E_g(3)$. The number in parentheses is the number of times a particular state occurs. The superscript indicates the spin multiplicity and A_1 , A_2 , B_1 , B_2 , E are the irreducible representations in D_{4h} symmetry according to how the orbital angular momentum transforms. In the presence of spin-orbit interaction, the spin angular momentum couples with the orbital angular momentum and the resultant states we will denote in the Bethe notation by Γ_i where i is 1–5. For 5d transition metal ions spin-orbit interaction cannot be neglected.⁸

Fenske, Martin, and Rudenberg⁹ have derived the appropriate matrix elements to describe the crystal

(9) R. F. Fenske, D. S. Martin, Jr., and K. Rudenberg, *Inorg. Chem.*, **1**, 441 (1962).

field, interelectronic repulsion, and spin-orbit interaction. The interelectronic repulsion results in matrix elements which are functions of the two Slater-Condon parameters F_2 and F_4 . The crystal field effect gives rise to matrix elements which are functions of the parameters Δ_1 , Δ_2 , and Δ_3 . In the strong field picture, Δ_1 is the energy difference between the $d_{x^2-y^2}$ orbital and the d_{xy} orbital, Δ_2 is the energy difference between the d_{xz} , d_{yz} orbitals and the $d_{x^2-y^2}$ orbital, and Δ_3 is the difference between the d_{z^2} orbital and the $d_{x^2-y^2}$ orbital.

Martin, Tucker, and Kassman¹⁰ have used the ref 9 matrix elements to perform crystal field calculations and have proposed two alternative energy-level schemes denoted as A and B. In alternative A the d-orbital ordering is $b_{1g} (d_{x^2-y^2}) > b_{2g} (d_{xy}) > e_g (d_{xz}, d_{yz}) > a_{1g} (d_{z^2})$ while in alternative B the $e_g (d_{xz}, d_{yz})$ and $a_{1g} (d_{z^2})$ orbitals have about the same energy. Recent MO calculations^{11,12} suggest alternative A is correct. The major difficulty with alternative B is that it was not possible to account for the band observed at 36,500 cm^{-1} in the reflectance spectrum of K_2PtCl_4 crystals by Day, *et al.*¹³ The difficulties with alternative A are several. First, for the band observed at 36,500 cm^{-1} , MTK were only able to fit with a calculated level at 35,300 cm^{-1} . Second, a state with moderate singlet character was calculated to be 22,000 cm^{-1} where no band could be observed. Finally, it was concluded by MTK that the calculated intensities were not consistent with the experimental data.

We have written a computer program to calculate from the ref 9 matrix elements the d^8 eigenvalues and eigenfunctions for given values of the parameters F_2 , F_4 , SO , Δ_1 , Δ_2 , and Δ_3 . The program was checked against the known calculations of MTK and in the limit that one or more of the parameters was zero. A prediction of the relative intensities was obtained by use of the spin intensity formula given by Schroeder.¹⁴ The crystal field analysis was carried out in several steps. First, computer graphs were made of the energies of the d^8 states as a function of a given parameter for fixed values of the other parameters. Next, by use of a successive approximation technique a number of sets of parameters were obtained which gave a reasonable fit energy wise to the available experimental data. However, the vibronic model for square-planar complexes² requires that $\Gamma_1 \rightarrow \Gamma_2$ and $\Gamma_1 \rightarrow \Gamma_4$ transitions be polarized in the x , y direction, whereas $\Gamma_1 \rightarrow \Gamma_1$, Γ_3 , Γ_5 transitions can occur with both x , y and z polarization. Consideration of the available polarization data^{2,3} narrowed the choice to one set of parameters which would describe the experimental data. In the final step, a least-squares computer program was used to give the best calculated fit to the experimental data.

In Table III the calculated and observed results are tabulated for two cases. In case I the observed experimental maxima have been fit to the crystal field model. Here, the root-mean-square deviation of the observed energies from the calculated energies is 11 cm^{-1} , well within the experimental uncertainty.

TABLE III
A COMPARISON OF THE OBSERVED AND CALCULATED ENERGIES FOR THE TETRACHLOROPLATINATE(II) ION

State	Energy calcd, cm^{-1}	Energy ^a obsd, cm^{-1}	Relative intensity Calcd
Case I: Crystal Field Fit to Observed Experimental Maxima ^b			
$\Gamma_1(^1A_{1g})$	0		
$\Gamma_1(^3E_g)$	16,013		3.2
$\Gamma_2(^3E_g)$	16,242		5.5
$\Gamma_3(^3E_g)$	17,039	17,060	3.4
$\Gamma_4(^3E_g)$	18,113	18,100	2.8
$\Gamma_5(^3E_g)$	18,960		4.6
$\Gamma_5(^3A_{2g})$	20,723	20,735	4.1
$\Gamma_1(^3A_{2g})$	21,198		5.5
$\Gamma_5(^3B_{1g})$	23,959	23,970	13.5
$\Gamma_4(^3B_{1g})$	25,276		3.0
$\Gamma_5(^3A_{2g})$	26,048	26,050	94.1
$\Gamma_5(^1E_g)$	29,569	29,575	82.6
$\Gamma_3(^1B_{1g})$	36,503	36,500	93.4
Case II: Crystal Field Fit to Observed Experimental Origins ^c			
$\Gamma_1(^1A_{1g})$	0		
$\Gamma_1(^3E_g)$	15,442		4.2
$\Gamma_2(^3E_g)$	15,872		7.8
$\Gamma_3(^3E_g)$	16,377	16,600	5.2
$\Gamma_4(^3E_g)$	17,537	17,400	3.9
$\Gamma_3(^3E_g)$	18,487		7.3
$\Gamma_5(^3A_{2g})$	19,509	19,500	6.8
$\Gamma_1(^3A_{2g})$	20,268		7.6
$\Gamma_5(^3B_{1g})$	22,839	22,880	26.6
$\Gamma_2(^1A_{2g})$	24,841	24,850	91.7
$\Gamma_4(^3B_{1g})$	24,893		4.1
$\Gamma_3(^1E_g)$	27,479	27,500	67.3
$\Gamma_3(^1B_{1g})$	32,995	33,000	90.7

^a Reference 3 average of x , y and z polarization data. ^b Parameters: $F_2 = 1406$, $F_4 = 54$, $SO = 1013$, $\Delta_1 = 25,961$, $\Delta_2 = 41,821$, and $\Delta_3 = 33,184 \text{ cm}^{-1}$. The root-mean-square (rms) deviation of the observed energies from the calculated energies is 11 cm^{-1} . ^c $F_2 = 920$, $F_4 = 69$, $SO = 1151$, $\Delta_1 = 25,368$, $\Delta_2 = 36,195$, and $\Delta_3 = 29,011 \text{ cm}^{-1}$. The rms deviation of the observed energies from the calculated energies is 101 cm^{-1} .

This is the type of analysis which MTK have performed. In case II the observed origin of each electronic transition has been fit to the crystal field model. In this case the rms deviation of the observed energies and the calculated energies is 101 cm^{-1} . Case II provides the more reasonable theoretical model but the problem is that there is considerable uncertainty in deciding where a given electronic transition begins.

The predicted intensities in either case I or case II are not in too good an agreement with the experimental intensity data. This is not too surprising since one should not expect to obtain a very good measure of intensity on the basis of "spin-allowedness" alone. For a discussion of the theory of intensity for vibronically allowed electric dipole transitions see Jordan, Patterson, and Dorain.¹⁵

Assignment of Vibronic Structure.—For d-d transitions in square-planar complexes both the initial and final electronic states are gerade so that in order for a transition to be allowed from one gerade state to another, intensity must be "borrowed" from an ungerade state via an odd vibrational mode. Thus, at 4°K the resolution is sufficient all vibronic structure should be ungerade. In Table IV selection rules are given that show which odd vibrational modes can mix with odd electronic states to make a given d-d transition with D_{4h} symmetry vibronically allowed. These results we

(10) D. S. Martin, M. A. Tucker, and A. J. Kassman, *Inorg. Chem.*, **5**, 1298 (1966).

(11) H. Basch and H. B. Gray, *ibid.*, **6**, 256 (1967).

(12) F. A. Cotton and C. B. Harris, *ibid.*, **6**, 369 (1967).

(13) P. Day, A. F. Orchard, A. J. Thomson, and R. J. P. Williams, *J. Chem. Phys.*, **42**, 1973 (1965).

(14) K. A. Schroeder, *ibid.*, **37**, 2553 (1963).

(15) P. C. Jordan, H. H. Patterson, and P. B. Dorain, *ibid.*, **49**, 3858 (1968).

TABLE IV
VIBRONIC SELECTION RULES FOR PtCl_4^{2-} COMPLEX SHOWING SYMMETRY OF THE VIBRATIONS ALLOWING d-d TRANSITIONS^a

Symmetry of final electronic state	Symmetry of initial vibrationless electronic state—				
	Γ_1	Γ_2	Γ_3	Γ_4	Γ_5
Γ_1	$a_{2u}(z)$ $e_u(xy)$	$e_u(xy)$	$b_{2u}(z)$ $e_u(xy)$	$e_u(xy)$	$e_u(z)$ $a_{2u}(xy)$ $b_{2u}(xy)$
Γ_2	$e_u(xy)$	$a_{2u}(z)$ $e_u(xy)$	$e_u(xy)$	$b_{2u}(z)$ $e_u(xy)$	$e_u(z)$ $a_{2u}(xy)$ $b_{2u}(xy)$
Γ_3	$b_{2u}(z)$ $e_u(xy)$	$e_u(xy)$	$a_{2u}(z)$ $e_u(xy)$	$e_u(xy)$	$e_u(z)$ $a_{2u}(xy)$ $b_{2u}(xy)$
Γ_4	$e_u(xy)$	$b_{2u}(z)$ $e_u(xy)$	$e_u(xy)$	$a_{2u}(z)$ $e_u(xy)$	$e_u(z)$ $a_{2u}(xy)$ $b_{2u}(xy)$
Γ_5	$e_u(z)$ $a_{2u}(xy)$ $b_{2u}(xy)$	$e_u(z)$ $a_{2u}(xy)$ $b_{2u}(xy)$	$e_u(z)$ $a_{2u}(xy)$ $b_{2u}(xy)$	$e_u(z)$ $a_{2u}(xy)$ $b_{2u}(xy)$	$e_u(xy)$ $a_{2u}(z)$ $b_{2u}(z)$

^a The notation z denotes absorption with the electric vector perpendicular to the PtCl_4^{2-} ionic plane, while xy refers to in-plane absorption. The notation is standard.

shall need for the assignment of the observed vibronic structure.

The normal modes of vibration for the PtCl_4^{2-} square-planar complex can be labeled $\nu_1(a_{1g})$, $\nu_2(b_{2g})$, $\nu_3(a_{2u})$, $\nu_4(b_{1g})$, $\nu_5(b_{2u})$, $\nu_6(e_u)$, and $\nu_7(e_u)$, where the irreducible representation of the D_{4h} point group according to how the mode transforms is given in parentheses. Table V gives the vibrational modes, activity,

TABLE V
GROUND-STATE VIBRATIONAL MODE ENERGIES, cm^{-1}

Mode	Activity	Motion	Cs_2PtCl_4	K_2PtCl_4
$\nu_1(a_{1g})$	Raman	Symmetric stretch		329 ^d
$\nu_2(b_{2g})$	Raman	In-plane bending		302 ^d
$\nu_3(a_{2u})$	Infrared	Out-of-plane bending	160, ^a 157 ^b	173 ^c
$\nu_4(b_{1g})$	Raman	Stretch		194 ^d
$\nu_5(b_{2u})$	Inactive	Out-of-plane bending		
$\nu_6(e_u)$	Infrared	Stretch	316, ^a 313 ^b	325 ^c
$\nu_7(e_u)$	Infrared	In-Plane bending	185, ^a 177 ^b	195 ^c

^a Reference 16. ^b Reference 17. ^c Reference 18. ^d P. J. Hendra, *Spectrochim. Acta, Part A*, **23**, 2871 (1967).

and vibrational energies reported to date for Cs_2PtCl_4 . Two values are listed for the infrared active vibrational modes of Cs_2PtCl_4 . The different values are the result of two independent investigations.^{16,17} The peak maxima are sufficiently broad to explain the differences. Raman active mode energies are not available for Cs_2PtCl_4 .

The argument for assignment of the luminescence spectrum has developed as follows. The average spacing between adjacent E peaks and between adjacent O peaks is 329 cm^{-1} . The value of the ν_1 symmetric stretch mode for Cs_2PtCl_4 from Raman studies is not known but the value of ν_1 for K_2PtCl_4 has been reported to be 329 cm^{-1} for the ground electronic state. If we visualize the luminescence as occurring by a transition from the zeroth vibrational levels of an excited

electronic state for PtCl_4^{2-} to the various vibrational levels of the ground electronic state then the observed luminescence peaks should correspond to the ground state vibrational modes. The values of ν_1 for the ground electronic states as calculated from the luminescence spectrum and as determined from Raman studies are in good agreement.

When the energy differences between the ground-state vibrational modes are compared with the spacings between the major experimental peaks, good agreement occurs only if we assign the O peaks to the ν_6 odd mode, the E peaks to the ν_3 odd mode, the B peaks to the ν_7 odd mode, of the ground electronic state $\Gamma_1(^1A_{1g})$. If ν_3 is 160 cm^{-1} , then ν_7 is 185 cm^{-1} , and ν_6 is 299 cm^{-1} . The L peaks, with a calculated energy of 30 cm^{-1} , are assigned to a lattice mode because the internal mode energies are expected to be greater than 100 cm^{-1} .¹⁸ Table VI is a listing of the observed

TABLE VI
ENERGIES AND ASSIGNMENTS FOR THE LUMINESCENCE SPECTRUM OF Cs_2PtCl_4 IN Cs_2ZrCl_6 AT 4°K

Peak no.	Energy, cm^{-1}	Assignment
10E	22,363	$\Gamma_5(^3B_{1g}) \rightarrow \Gamma_1(^1A_{1g}) + \nu_3$
9O	22,214	+ ν_6
9L	22,162	+ ($\nu_1 + \nu_L$)
9E	22,033	+ ($\nu_1 + \nu_3$)
9B	21,998	+ ($\nu_1 + \nu_7$)
8O	21,891	+ ($\nu_1 + \nu_6$)
8L	21,830	+ ($2\nu_1 + \nu_L$)
8E	21,706	+ ($2\nu_1 + \nu_3$)
8B	21,682	+ ($2\nu_1 + \nu_7$)
7O	21,561	+ ($2\nu_1 + \nu_6$)
7L	21,504	+ ($3\nu_1 + \nu_L$)
7E	21,374	+ ($3\nu_1 + \nu_3$)
7B	21,344	+ ($3\nu_1 + \nu_7$)
6O	21,235	+ ($3\nu_1 + \nu_6$)
6L	21,174	+ ($4\nu_1 + \nu_L$)
6E	21,046	+ ($4\nu_1 + \nu_3$)
6B	21,020	+ ($4\nu_1 + \nu_7$)
5O	20,910	+ ($4\nu_1 + \nu_6$)
5L	20,860	+ ($5\nu_1 + \nu_L$)
5E	20,719	+ ($5\nu_1 + \nu_3$)
5B	20,696	+ ($5\nu_1 + \nu_7$)
4O	20,580	+ ($5\nu_1 + \nu_6$)
4L	20,521	+ ($6\nu_1 + \nu_L$)
4E	20,388	+ ($6\nu_1 + \nu_3$)
4B	20,369	+ ($6\nu_1 + \nu_7$)
3O	20,251	+ ($6\nu_1 + \nu_6$)
3L	20,194	+ ($7\nu_1 + \nu_L$)
3E	20,060	+ ($7\nu_1 + \nu_3$)
3B	20,028	+ ($7\nu_1 + \nu_7$)
2O	19,923	+ ($7\nu_1 + \nu_6$)
2L	19,874	+ ($8\nu_1 + \nu_L$)
2E	19,735	+ ($8\nu_1 + \nu_3$)
1O	19,599	+ ($8\nu_1 + \nu_6$)
1E	19,406	+ ($9\nu_1 + \nu_3$)

energies and assignments for the major luminescence peaks.

In the lower energy end of the luminescence spectrum additional sharp peaks appear. One explanation for this is as follows. The crystal structure of Cs_2ZrCl_6 is an antifluorite cubic arrangement with four Cs_2ZrCl_6 units per unit cell with a unit cell length of 10.428 \AA .¹⁹ This may be pictured as a cubic lattice of cesium ions in which every other body-centered position is occupied by a ZrCl_6^{2-} ion. When PtCl_4^{2-} substitutes for ZrCl_6^{2-}

(16) A. Sabatini, L. Sacconi, and V. Schettino, *Inorg. Chem.*, **3**, 1775 (1964).

(17) J. H. Fertel and C. H. Perry, *J. Phys. Chem. Solids*, **26**, 1773 (1965).

(18) J. R. Ferraro, *J. Chem. Phys.*, **53**, 117 (1970).

(19) J. D. H. Donnay and G. Donnay, Ed., "Crystal Data Determination Tables," 2nd ed, American Crystallographic Association, New York, N. Y., 1963.

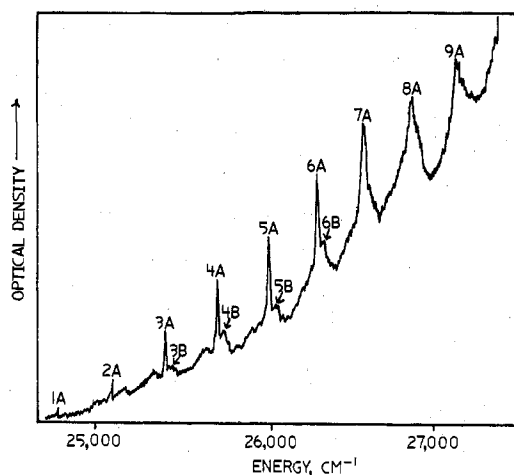


Figure 5.—Microphotometer tracing of the $\Gamma_1(^1A_{1g}) \rightarrow \Gamma_2(^1A_{2g})$ transition showing a detailed vibronic absorption spectrum for a $\text{Cs}_2\text{PtCl}_4\text{-Cs}_2\text{ZrCl}_6$ crystal at 4°K.

it is quite possible that all the PtCl_4^{2-} ions do not have perfect cubic site symmetry. In this case, as transitions occur into the ground electronic state with more quanta of the ν_1 symmetric stretch mode excited, the complex samples to a greater extent its surroundings, and ions with slightly less than cubic site symmetry give rise to additional peaks.

On the basis of the luminescence spectrum assignments the origin of the transition is calculated to be 22,523 cm^{-1} . In contrast, the origin of the band 4 transition observed in pure K_2PtCl_4 crystals occurs between 22,550 and 22,750 cm^{-1} depending upon the assignment of peak A in Figure 2. If it is assumed that a shift of about -50 cm^{-1} occurs in going from the pure potassium salt to the cesium salt doped in Cs_2ZrCl_6 , as observed for the $\Gamma_1(^1A_{1g}) \rightarrow \Gamma_2(^1A_{2g})$ transition, then one may conclude that the band 4 absorption spectrum and the luminescence spectrum both arise from the same system.

The vibronic selection rules in Table IV show that the luminescence results from either a $\Gamma_1 \rightarrow \Gamma_1$ or a $\Gamma_5 \rightarrow \Gamma_1$ electronic transition because of the appearance of e_{1u} and a_{2u} modes in the spectrum. For a $\Gamma_5 \rightarrow \Gamma_1$ transition the selection rules predict the appearance also of the b_{2u} vibrational mode. Unfortunately, the b_{2u} mode is Raman and infrared inactive so that the mode energy for Cs_2PtCl_4 has not been measured. Force constant calculations of Fertel and Perry¹⁷ give an estimated value of about 120 cm^{-1} for $\nu_5(b_{2u})$. No emission peaks appear at this energy; however, it is possible the b_{2u} mode is present as a shoulder on the E peaks at about 130 cm^{-1} . In the unlikely but possible situation that the b_{2u} out-of-plane bending mode and the a_{2u} out-of-plane bending mode have the same energy a $\Gamma_3 \rightarrow \Gamma_1$ assignment for the emission spectrum cannot be excluded (see Table IV). In any case, the $\Gamma_5(^3B_{1g}) \rightarrow \Gamma_1(^1A_{1g})$ crystal field assignment is in agreement with the vibronic selection rules. Also, the MTK alternative B assignment $\Gamma_1(^3B_{1g}) \rightarrow \Gamma_1(^1A_{1g})$ is in agreement.

For the $\Gamma_1(^1A_{1g}) \rightarrow \Gamma_2(^1A_{2g})$ absorption spectrum observed between 24,800 and 28,000 cm^{-1} , and shown in Figure 5, analysis of the vibronic peaks is made as follows. To the right of several of the A peaks are much smaller, broader peaks designated by the letter B. The B peaks can be seen on the original photographic

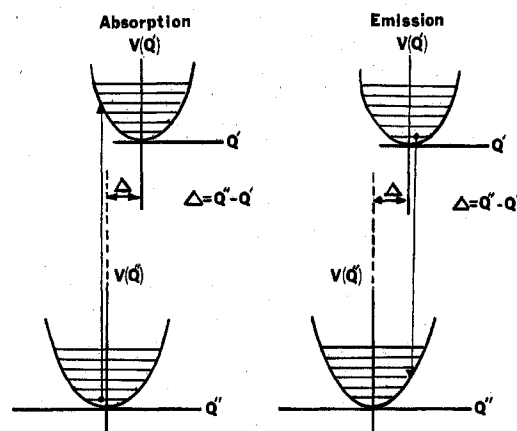


Figure 6.—Harmonic oscillator potential well diagrams.

plates. The average spacing between the A peaks and the B peaks is 40 cm^{-1} . The A peaks are assigned to the ν_6 mode and the B peaks to the ν_L lattice mode. If the ν_L lattice mode is assumed to be 30 cm^{-1} , then ν_6 for the $\Gamma_2(^1A_{2g})$ excited state is 283 cm^{-1} in contrast to the value of 299 cm^{-1} for the $\Gamma_1(^1A_{1g})$ ground state calculated from the luminescence spectrum. The value of the ν_1 symmetric stretch mode of 293 cm^{-1} for the $\Gamma_2(^1A_{2g})$ state is somewhat less than the ground state value of 329 cm^{-1} . All of the peak assignments are given in Table VII.

TABLE VII
OBSERVED OPTICAL TRANSITIONS IN THE 24,800–28,000- cm^{-1}
ENERGY REGION FOR PtCl_4^{2-} IN Cs_2ZrCl_6 AT 4°K

Peak	Energy, cm^{-1}	Relative intensity ^a	Assignment
1A	24,800	S	$\Gamma_2(^1A_{2g}) + \nu_6$
2A	25,097	S	+ ($\nu_1 + \nu_6$)
3A	25,392	S	+ ($2\nu_1 + \nu_6$)
3B	25,429	W	+ ($3\nu_1 + \nu_L$)
4A	25,688	S	+ ($3\nu_1 + \nu_6$)
4B	25,723	W	+ ($4\nu_1 + \nu_L$)
5A	25,975	S	+ ($4\nu_1 + \nu_6$)
5B	26,014	W	+ ($5\nu_1 + \nu_L$)
6A	26,270	S	+ ($5\nu_1 + \nu_6$)
6B	26,318	W	+ ($6\nu_1 + \nu_L$)
7A	26,571	S	+ ($6\nu_1 + \nu_6$)
8A	26,857	S	+ ($7\nu_1 + \nu_6$)
9A	27,140	S	+ ($8\nu_1 + \nu_6$)
10A	27,423	S	+ ($9\nu_1 + \nu_6$)
11A	27,716	S	+ ($10\nu_1 + \nu_6$)
12A	28,003	S	+ ($11\nu_1 + \nu_6$)

^a S means strong and W means weak relative intensity.

Franck-Condon Analysis of the Luminescence Spectrum.—The Franck-Condon principle can be stated as follows: an electronic transition in a molecular complex takes place so rapidly in comparison to the vibrational motion that immediately afterwards the nuclei still have very nearly the same relative position and velocity as before the transition.

In Figure 6, the potential curves of two electronic states have been drawn so that the minimum of the upper potential curve lies at a greater r value than of the lower potential curve. In absorption studies at 4°K, the complex is initially at the minimum of the lower potential curve. Thus, on the basis of the Franck-Condon principle the most probable transition is from $v'' = 0$ to $v' > 0$ (vertically upwards). For this transition there is no change in the internuclear

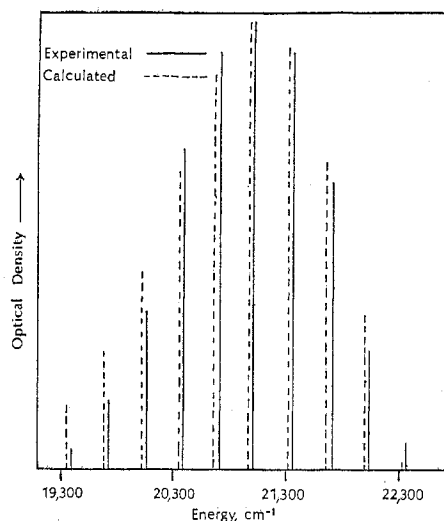


Figure 7.—Comparison of calculated and measured relative intensities for the luminescence spectrum of a $\text{Cs}_2\text{PtCl}_4\text{-Cs}_2\text{ZrCl}_6$ single crystal at 4°K .

distance at the moment of the transition and no change in the velocity of the nuclei. Immediately after the transition the nuclei still have the same relative distance from each other. Since the equilibrium internuclear value is greater in v' than v'' the nuclei begin to vibrate after the transition.

The variation of intensity in a band progression in emission from $v' = 0$ corresponds exactly to that of a progression from $v'' = 0$ in absorption; that is, there is an intensity maximum at a v'' value that is determined by the relative position of the minima of the two potential curves. The greater the difference of the r_e values the greater is the v'' value of the intensity maximum.

Various workers have described approximate methods for quantitatively applying the Franck-Condon principle to study the geometry of an excited electronic state. To calculate the various overlap integrals in the harmonic oscillator approximation, the vibrational wave functions for the ground electronic state and for the excited electronic state have to be expressed in terms of Hermite polynomials. Henderson, *et al.*,²⁰ have developed a method to evaluate, in dimensionless form convenient for numerical computation, Franck-Condon overlap integrals in terms of B , the ratio of the ground to excited state vibrational frequencies,

(20) J. R. Henderson, M. Muramoto, and R. A. Willett, *J. Chem. Phys.*, **41**, 580 (1964).

and Δ , the ratio of the displacement of the ground and excited state normal coordinates.

The energies and the relative intensities of the E peaks in the luminescence spectrum were measured and the parameters varied until the theoretical intensities matched best the experimental intensities. The value of ν_1 for the ground electronic state was taken to be 329 cm^{-1} from the luminescence data. The value of ν_1 for the excited electronic state was taken to be 298 cm^{-1} from the K_2PtCl_4 absorption data. The value of Δ calculated from the Franck-Condon analysis was -0.159 \AA . In Figure 7 bar graphs are given comparing the experimental and theoretical intensities. The standard deviation is 5 units on a scale of 100 units.

Summary.—It has been shown in this paper that the optical spectrum of potassium tetrachloroplatinate(II) can be understood on the basis of a $5d^8$ ion with square-planar symmetry. The calculated energies based on a crystal field model, with orbital energies $d_{x^2-y^2} > d_{xy} > d_{z^2}$, $d_{yz} > d_{z^2}$, fit the observed energies with an rms deviation of about 100 cm^{-1} .

When the tetrachloroplatinate(II) ion is doped into cesium hexachlorozirconate(IV) a very detailed and complicated luminescence spectrum is observed at 4°K . The vibronic structure consists of progressions in the symmetric stretch mode coupled to odd vibrational modes of the PtCl_4^{2-} complex. This spectrum should be compared with the simple sharp-line luminescence results we have recently reported at 20°K for the $5d^3$ hexabromorhenate(IV) ion doped into cesium hexabromozirconate(IV).²¹

Work is presently under way to grow mixed crystals with a sufficient amount of the tetrachloroplatinate(II) ion so as to be able to detect the weak spin-forbidden transitions. It is hoped that magnetic measurements can be made in the future for the luminescence spectrum to confirm and extend our analysis.

Acknowledgments.—This research has been supported in part by a Frederick Gardner Cottrell Grant from the Research Corporation and in part by a grant from the Faculty Research Fund of the University of Maine at Orono. We especially wish to thank Professor Paul Dorain for the use of his spectroscopic equipment in the early stages of this investigation. The computations reported herein were performed at the University of Maine Computation Center.

(21) H. H. Patterson, J. L. Nims, and C. M. Valencia, *J. Mol. Spectrosc.*, **42**, 567 (1972).